Check for updates

View Article Online
View Journal

Journal of Materials Chemistry C

Accepted Manuscript

This article can be cited before page numbers have been issued, to do this please use: C. Liu, H. Wang, J. Du, K. Zhao, P. Hu, B. Wang, H. Monobe, B. Heinrich and B. Donnio, *J. Mater. Chem. C*, 2018, DOI: 10.1039/C7TC05315K.

Volume 4 | Number 1 | 7 January 2016 | Pages 1–224

Journal of
Materials Chemistry C

Materials for optical, magnetic and electronic devices
www.rsc.org/MaterialsC

ISSN 2050-7526

ROYAL SOCIETY OF CHEMISTRY

PAPER
Nguyễn T. K. Thanh, Xiaodi Su *et al.*
Fine-tuning of gold nanorod dimensions and plasmonic properties using the Hofmeister effects

175 YEARS

This is an Accepted Manuscript, which has been through the Royal Society of Chemistry peer review process and has been accepted for publication.

Accepted Manuscripts are published online shortly after acceptance, before technical editing, formatting and proof reading. Using this free service, authors can make their results available to the community, in citable form, before we publish the edited article. We will replace this Accepted Manuscript with the edited and formatted Advance Article as soon as it is available.

You can find more information about Accepted Manuscripts in the author guidelines.

Please note that technical editing may introduce minor changes to the text and/or graphics, which may alter content. The journal's standard Terms & Conditions and the ethical guidelines, outlined in our author and reviewer resource centre, still apply. In no event shall the Royal Society of Chemistry be held responsible for any errors or omissions in this Accepted Manuscript or any consequences arising from the use of any information it contains.

ROYAL SOCIETY OF CHEMISTRY

rsc.li/materials-c

View Article Online
DOI: 10.1039/C7TC05315K

Journal Name

ARTICLE

Molecular Design of Benzothienobenzothiophene-Cored Columnar Mesogens: Facile Synthesis, Mesomorphism, and Charge Carrier Mobility

Received 00th January 20xx,
Accepted 00th January 20xx

DOI: 10.1039/x0xx00000x

www.rsc.org/

Chun-Xia Liu,[a] Hu Wang,[a] Jun-Qi Du,[a] Ke-Qing Zhao[a*], Ping Hu,[a] Bi-Qin Wang,[a] Hirosato Monobe,[b*] Benoît Heinrich,[c] Bertrand Donnio,[c*]

Benzothienobenzothiophene (BTBT) liquid-crystalline semiconductors are arousing a lot of interest due to their long-range ordered, self-organizational abilities and high-charge carrier transport properties. In this work, we report the design and the straightforward synthesis of a homologous series of compounds containing the BTBT substructure by the successive Suzuki cross-coupling and $FeCl_3$ oxidative Scholl cyclodehydrogenation reaction. The target π-conjugated aromatic, H-shaped sanidic mesogens self-organize into a classical hexagonal columnar mesophase over wide temperature ranges as deduced from polarized optical microscopy (POM), differential scanning calorimetry (DSC), and small-angle X-ray scattering (SAXS) investigations. UV/Vis absorption and photoluminescent spectra, measured in both solution and film, revealed strong photoluminescence with high quantum yields. The charge carrier mobility measured by time-of-flight (TOF) technique showed a balanced ambipolar hole and electron mobility in the range of 10^{-3} cm^2 V^{-1} s^{-1} between 100 to 230°C in the mesophase. These BTBT-based columnar liquid crystals may represent attractive candidates to be incorporated within one-dimensionnal organic optoelectronic devices.

Introduction

Thiophene-based materials are ubiquitous as organic semiconductors.[1-6] The sulfur-containing aromatic heterocycle possesses a versatile and unique chemistry, and the investigation of thiophene-containing oligomers,[7] dendrimers[8] and polymers,[9] as well as polycyclic aromatics[1-6] are becoming a vivid part of contemporary chemistry, including synthetic and materials chemistries. Potentially more interesting, are the related two-dimensional, conjugated thiophene-fused aromatics.[10-22] They have been found to prefer ordered arrangements stabilized by π-π intermolecular interactions with large molecular orbital overlaps, which result in the enhancement of the charge carrier mobility. As such, these fused thiophene molecular materials are being extensively investigated in organic thin-film electronics and optoelectronic devices such as organic field-effect transistors (OFETs),[10] photovoltaic solar cells (OPVs),[11] and light-emitting diodes (OLEDs).[12]

Compared with crystalline and amorphous molecular semiconducting materials, mesomorphous semiconductors combine features of both, i.e. self-organizational tendency, fluidity and molecular dynamics which help to self-heal defects, and high charge carrier mobility.[23-28] Molecular design and straight synthesis of novel mesophase semiconductors are highly desirable due to their controllable anisotropy with one- or two-dimensional charge transport property and outstanding thin-film device performance.[26,27]

Among the large amount of S-containing aromatics reported so far in the literature, benzothienobenzothiophene (BTBT) derivatives have been found to display lamellar columnar mesophases,[29] as well as high ordered layered smectic mesophases.[30-32] The former systems show time-of-flight (TOF) charge drift mobility in 10^{-3} cm^2 V^{-1} s^{-1} range, whereas the latter ones display higher TOF mobility as well as excellent OFET device' performances in their high ordered crystalline phase, which is templated by slowly cooling from the fluid high-temperature smectic liquid crystalline phase,[32] or just by solution process.[31]

However, discotic columnar mesomorphic materials possess one-dimensional π-π stacked columnar mesophase, and charge carriers hopping along the discotic columns, whereas the peripheral alkyl chains play the role of insulator. Such supramolecular columns appear therefore as ideal one-dimensional pathway for charge carrier transport.[33-36] The charge carrier mobility, according to Marcus's electronic transfer theory of small molecules,[37] is determined mainly by two parameters: the reorganization energy and the charge transfer integral, both parameters being related to the

---

[a] College of Chemistry and Material Science, Sichuan Normal University, Chengdu 610066, China. E-mail: kqzhao@sicnu.edu.cn
[b] Inorganic Functional Materials Research Institute, National Institute of Advanced Industrial Science and Technology (AIST), Ikeda, Osaka 5638577, Japan. E-mail: monobe-hirosato@aist.go.jp
[c] Institut de Physique et Chimie des Matériaux de Strasbourg (IPCMS), CNRS-Université de Strasbourg (UMR 7504), 67034 Strasbourg, France. E-mail: bertrand.donnio@ipcms.unistra.fr

Electronic Supplementary Information (ESI) available: Experimental techniques, synthetic details, ^{1}H NMR, HMRS, POM, DSC, TGA, SAXS, indexation tables. See DOI: 10.1039/x0xx00000x

View Article Online
DOI: 10.1039/C7TC05315K

molecular chemical structure and to the molecular packing morphology in mesophase.[38] Therefore, it is expected that BTBT-containing columnar mesogens are also suitable candidate for one-dimensional mesophase semiconductors.

BTBT derivatives with 2,7-disubstitution normally exhibit smectic phases,[30-32] but the synthesis of BTBT-cored compounds with six to eight peripheral alkyl chains to induce discotic columnar mesophase is still regarded as challenging. The construction of useful mesophase semiconductors by higher efficient synthetic methods is a crucial objective,[39-44] and introducing BTBT-unit into discotic columnar mesophase would provide a new and exciting class of one-dimensional semiconductor materials.

Here, we report the design and the straightforward synthesis of BTBT-unit containing columnar mesogens by two different synthetic routes involving either intermolecular or intramolecular $FeCl_3$ oxidative Scholl cyclodehydrogenation reaction as key step reactions (Scheme 1). Both approaches have their own assets and specificities. The intermolecular cross-oxidative Scholl reaction is a linear strategy (Route 1, Scheme 1) specifically dedicated for the construction of unsymmetrical BTBT-containing compounds, i.e. with a "Janus" structure, by, for example, associating similar building block, but bearing alkyl chains of different lengths, of by combining hydrophilic/hydrophobic or fluorophilic/fluorophobic peripheries, which would impact on their self-assembly, thermal, solubility and surface properties. It is nonetheless a time-consuming solution, as it also requires tedious purifications. The intramolecular approach (Route 2, Scheme 1) is more direct and straightforward, and highly efficient to produce symmetrical structures by orthogonal coupling in high yield, with also much simpler purification processes. All the BTBT-containing molecules prepared thereafter are symmetrical, and the homogeneous alkyl periphery was increased from pentyl to dodecyl chains to tune the liquid crystalline temperature ranges and transition temperatures. The liquid crystalline properties of these compounds have been carefully investigated by POM, DSC, and SAXS. Their optical properties (UV/Vis absorption and photoluminescence) measured in both solution revealed strong photoluminescence with high quantum yields. Furthermore, the charge carrier mobility of one representative material, measured by the time-of-flight (TOF) transient photocurrent technique, exhibited ambipolar hole and electron drift mobility above 10^{-3} cm^2 V^{-1} s^{-1}, showing a great potential as mesomorphous semiconductors.

Results and Discussion

Methodology, Synthesis and Characterization

The two different synthetic methods were tested with success for the fabrication of the H-shape fused thiophenes, **M1**-**5**: the intermolecular cross-oxidative Scholl reaction afforded compound **M1** (Route 1, Scheme 1), whereas the other terms of the series, **M2**-**5**, were obtained in high yields by the direct intramolecular cross-oxidative Scholl reaction (Route 2, Scheme 1).

The preparation of **M1** was achieved in three steps, starting from precursory biphenylene derivatives (Supplementary Information, SI, and in reference 35), and consisted of the Suzuki coupling between thieno[3,2-b]thiophen-2-ylboronic acid and the 2-bromo-1,1'-biphenyl precursor (**1-1**) to yield the key precursor **1-2** (75%), followed by a first $FeCl_3$ oxidation to yield **1-3** in 81%, which was then immediately reacted with 3,3',4,4'-tetra(pentyloxy)biphenyl by the second $FeCl_3$ oxidative cross coupling to yield **M1** in 43% yield. The cross-cyclodehydrogenation resulted in 4 C-H bonds cleavage and two C-C bond formation in one-pot, which is highly efficient. This multiple-step synthetic method is however time-consuming (three steps), affords a low overall yield (26%), and the isolation of the pure target compounds was difficult, and systematically required several purifications by column chromatography. Despite the repeated purification procedures, this strategy is nevertheless very interesting and could be implemented to the synthesis of unsymmetrical BTBT-based "Janus" mesogens decorated by aliphatic chains of different lengths or by chains of different chemical natures, when, for example different functional biphenyls are used, of relevance for the construction of original self-assembled functional materials.

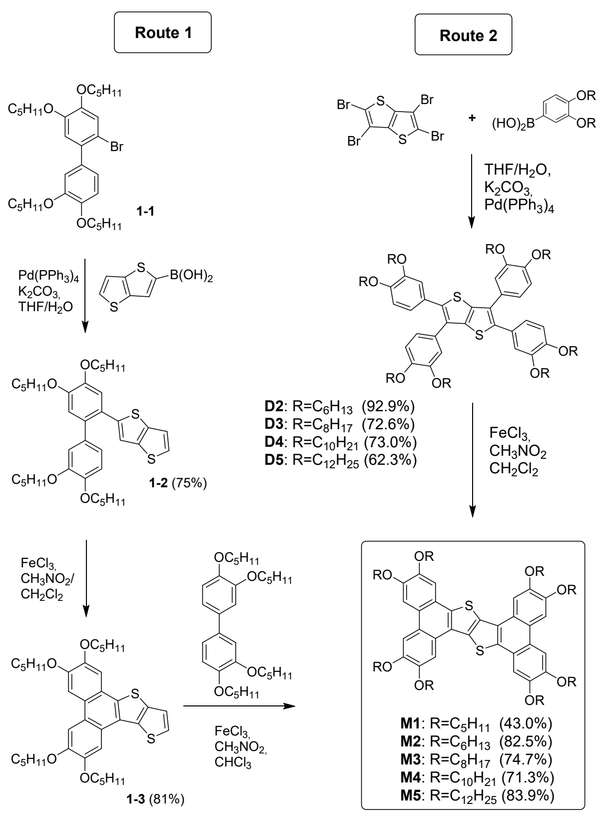

Scheme 1. Synthesis of the fused thieno[3,2-b]thiophene H-shaped liquid crystals, and precursors (**D2**-**5**), by Suzuki coupling and i) intermolecular (Route 1, **M1**) or ii) intramolecular (Route 2, **M2**-**5**) Scholl cyclodehydrogenation reaction, nomeclature, and yields (Details shown in SI).

As for the next terms of the series with longer peripheral chains, they were prepared in two steps, starting from

View Article Online
DOI: 10.1039/C7TC05315K

tetrabromothieno[3,2-b]thiophene (obtained in quantitive yields from direct bromination of thieno[3,2-b]thiophene in excess of bromine, Scheme S1) by Suzuki cross-coupling with various 3,4-dialkoxyphenyl)boronic acids to yield the corresponding tetraarylthieno[3,2-b]thiophenes **D2**-**5** (62-93%). Oxidative cyclodehydrogenation of **D2**-**5** by $FeCl_3/MeNO_2$ produced the target fused mesogens **M2**–**5** in good yields (71~84%). The compounds were isolated by simple filtration and purified by crystallization, without tedious column chromatography purifications. It is stressed that this intramolecular cyclodehydrogenation resulted in 4 C-H bonds cleavage and two C-C bond formation in one-pot, and no isomeric compounds were isolated, as confirmed by ^{1}H-NMR (Figures S25-29, SI).

All the **D** and **M** (and some intermediate) compounds were characterized by ^{1}H NMR (Figures S11-S29, SI) and the fused compounds (**M1**-**5**) were further analyzed by high resolution mass spectra (HRMS, Figures S30-S34, SI). The results were in agreement with the molecular structures. Detailed synthesis of all precursors is given in SI.

Thermal stability and Mesomorphism TGA, DSC, POM

The thermal stability of the targeted H-shaped sanidic mesogens was measured by thermal gravimetric analysis (TGA): compounds **M2**-**5** exhibited very high thermal stability, displaying thermal decomposition temperatures higher than 380°C (Figure S5, SI). The thermal behavior and liquid crystalline properties of intermediates **1**-*n* and **D2**-**5** and target compounds **M1**-**5** (Table 1) were investigated by polarized optical microscopy (POM, Figures S1-2, SI) and by differential scanning calorimetry (DSC, Figures S3-4, SI). As expected from some previous work, neither compounds **1**-**2** and **1**-**3**,[35] nor any of the precursory compounds **D2**-**5** were mesomorphous, whereas all final compounds exhibit mesomorphism, over large temperature ranges (Figure S4, SI). The sanidic compounds display typical fan-shaped optical textures, long linear defects and large homeotropic domains (Figure S2, SI), which are characteristics of a hexagonal columnar mesophase.

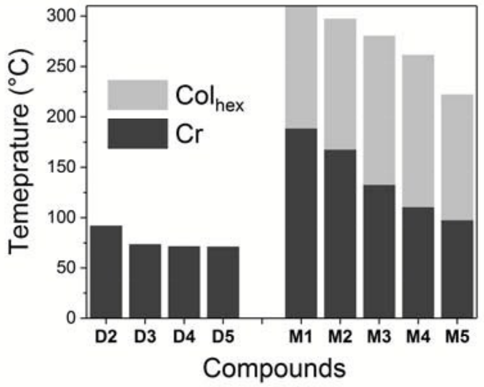

Figure 1. Phase diagram of BTBT-cored mesogens **M** and of their non-mesomorphic precursors **D**.

Apart from **D2**, the other tetraarylthioeno[3,2-b]thiophenes exhibit a complex solid state behavior, with the formation of a metastable solid phase on cooling the samples from the isotropic liquid, that crystallizes on subsequent heating (cold crystallization). The isotropization temperature is also found to decrease with chain-length (Figure 1, Table 1). The rapid rotation around the sigma bond axis of the four appending bulky dialkoxyaryl units connected to the central thieno[3,2-b]thiophene is thought to be the main cause for this solid-state thermal behavior and for the absence of mesomorphism in this series, as probably detrimental to cohesive stacking into columns.

After cyclodehydrogenation, the substituted phenyls and the central thieno[3,2-b]thiophene core fuse into a large, co-planar π-conjugated discotic aryl-containing molecule. Consequently, the self-organization process is strongly affected, and an enantiotropic Col$_{hex}$ mesophase (SAXS) is induced for all **M1**-**5** compounds, at rather elevated temperatures though, consistent with stronger π-π intermolecular interactions and the substantial increase of the isotropization temperatures (by more than 200°C on average, Figure 1) with respect to the corresponding **D** terms: the I-to-Col$_{hex}$ transition temperatures is maximal for **M1** (309°C) and continuously decreases in the series with the dilution of the mesogenic cores, down to 226°C as the peripheral chain length increases to dodecyl. Melting also decreases steadily with chain-length. The variation of the chain lengths proved a maximum extension of the mesomorphous range for the derivatives with eight octyl and decyl side chains, **M3** and **M4** (Table 1).

Table 1. Mesophases, transition temperatures and enthalpy changes for compounds **D** and **M** (heating and cooling rate of 5-10 °C·min^{-1})[a]

	Second heating [first cooling] / °C (ΔH, kJ·mol^{-1})
D2	Cr 91.8(87.5) I [I 73.1(-85.7) Cr]
D3	Cr* 44(-~40) Cr 57.0(-) Cr’ 73.5(74.3) I [I 65.4(-20.8) Cr’ 53.0(-) Cr*]
D4	Cr* 44(-50.0) Cr 71.4(122.2) I [I 52.5(-11.1) Cr 41(-25) Cr*]
D5	Cr 8(11.0) Cr* 38(-60.0) Cr’ 71(130.5) I [I 48(-64.1) Cr’ 1(-8.0) Cr]
M1	Cr 111(5.0) Cr’ 179(-) Cr” 189(29.6)† **Col$_{hex}$** 309(6.8) I [I 307(-6.2) **Col$_{hex}$** 161(-24.3) Cr 90(-10.0) Cr’]
M2	Cr 125(4.0) Cr’ 161(-) Cr” 168(14.7)† **Col$_{hex}$** 297(8.4) I [I 295(8.5) **Col$_{hex}$** 150(-34.7) Cr’ 122(-4.0) Cr]
M3	Cr 109(-) Cr’ 125(-) Cr” 133(11.5)† **Col$_{hex}$** 280(6.1) I [I 279(-3.4) **Col$_{hex}$** 107(56.9) Cr’ 97(-) Cr]
M4	Cr -11(4.0) Cr’ 104(-) Cr” 111(44)† **Col$_{hex}$** 261(9.7) I [I 260(-9.7) **Col$_{hex}$** 87(96.2) Cr’ -10(-) Cr]
M5	Cr 79(55.0) Cr’ 98(56.7) **Col$_{hex}$** 226(4.5) I [I 222(-4.1) **Col$_{hex}$** 61(-127.7) Cr]

[a] Cr, Cr’, Cr”: crystalline phases; Cr*: metastable crystalline phase, or mixture of (partially or conformationnally disordered) crystalline and amorphous solids; Col$_{hex}$: hexagonal columnar mesophase; I: isotropic liquid. †Cumulated enthalpy.

View Article Online
DOI: 10.1039/C7TC05315K

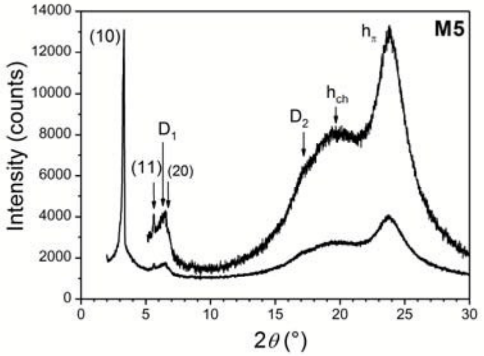

Figure 2. Representative SAXS pattern of compounds **M** (**M5** at 180°C)

Characterization of the mesophase by small-angle X-ray scattering (SAXS)

The SAXS patterns were recorded for all samples, at various temperatures (Figures 2 and S6-9, Tables 2 and S1). The absence of mesomorphism was confirmed for compounds **D2**-**5**. In these cases, the SAXS patterns, recorded below the isotropic phase, revealed a crystalline phase for **D2**, and the co-existence of crystalline and amorphous phases (for **D3**-**5**), in agreement with their complex thermal behavior detected by DSC (and POM). On the contrary, all the fused thieno[3,2-b]thiophene compounds self-organize into a Col$_{hex}$ mesophase at high temperature, constituted by supramolecular columns of stacked mesogens (spacing from scattering signal: h_π = 3.73-3.82 Å, Figure 2), arranged at the nodes of a hexagonal array, and separated from each other by a continuum of molten chains (liquid-like lateral distances between molten chains, ch, from broad maximum: $h_{ch} \approx 4.5$ Å, Figure 2). The long-range correlated two-dimensional columnar lattices are characterized by a relatively large number of reflections and thus by quite sharp interfaces with the continuum, obviously in relation with a strongly cohesive stacking (five reflections (*hk*) visible for **M1**/**M2** and still three for the longest chain homologues **M4**/**M5**, Table S1, Figures 2, S6-9). The cause might be the reinforced interactions from thienothiophene segments, whose presence further confers an ovoid shape and zones devoid of side-chains to mesogens. Yet, the hexagonal symmetry implies that columns have an average cylindrical shape with a regular distribution of aliphatic tails along their periphery. The mesogens must therefore adopt various (non-preferential) orientations along the stacking directions and be tilted

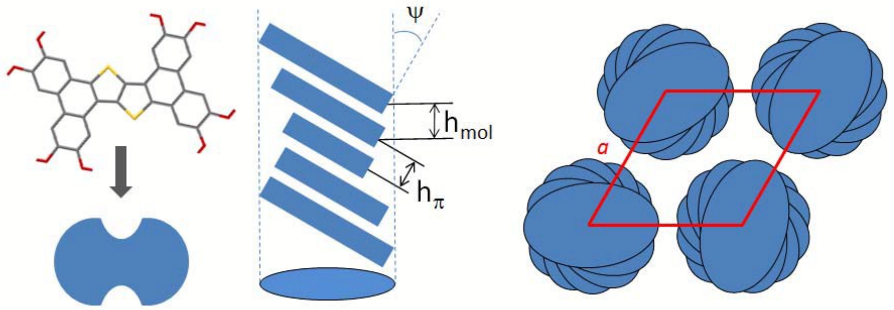

Figure 3. Stacking features and supramolecular model of the fused thieno[3,2-b]thiophene cores stacked into cylindrical columns, with tilt and non-preferential orientations of the mesogen cores (in blue); hexagonal lattice in red (Models were reconstructed from single crystal structures of 2,3,6,7,10,11-hexaethoxytriphenylene (CSD-XEFTAD),[49] and thieno[3,2-b]thiophene (CSD-THIPHT)[50]). The molten chains continuum between the columns is not shown for clarity.

Table 2. Mesophase parameter of the Col$_{hex}$ of compounds **M1-5**†

Cpds	T	V_{mol}	ρ	χ_{Vch}	a	$A[Z]$	h_{mol}	h_π	ψ	A_{core}	D_{cyl}	$S_{ch,cyl}$	$q_{ch,cyl}$
M1	240	1982	0.95	0.62(2)	23.5	478[1]	4.14	3.76	25	181	15.2	24.7	1.02
M2	230	2258	0.91	0.66(4)	23.7	488[1]	4.60	3.82	34	165	14.5	26.2	1.07
M3	210	2722	0.90	0.72(5)	26.7	616[1]	4.48	3.76	33	167	14.6	25.7	1.06
M4	200	3194	0.88	0.76(7)	28.4	700[1]	4.64	3.76	36	161	14.3	26.0	1.08
M5	180	3635	0.88	0.79(8)	31.3	847[1]	4.45	3.73	33	165	14.5	25.3	1.07

†T, temperature of the measure in °C; V_{mol}, molecular volume (Å^3) and, ρ, density (g cm^{-3}) calculated from partial volumes of reference substances (accuracy ca. 4%); $\chi_{V,ch}$, aliphatic volume fraction ($\chi_{V,ch} = V_{ch}/V_{mol}$); lattice parameter ($a$, Å), area ($A = 2a^2/\sqrt{3}$, Å^2) and Z, number of columns par lattice ($Z = 1$); columnar slice thickness (Å) $h_{mol} = V_{mol}/(Z{\times}A)$; h_π, stacking distance from SAXS pattern (missing value for **M*n*** terms was estimated to ca. 3.8 Å); ψ, out-of- plane tilt angle of mesogens inside columns $\psi = \arccos(h_\pi/h_{mol})$ (°); A_{core}, cross-sectional area of columnar cores (Å^2): $A_{core} = \chi_{Vch}A/Z$; D_{cyl} (Å), diameter of equivalent cylinder of cross-sectional area A_{core}; $S_{ch,cyl}$, cylinder area per chain (Å^2): $S_{ch,cyl} = \pi D_{cyl}{\times}h_{mol}/n_{ch}$, n_{ch} being the number of chains per molecule ($n_{ch} = 8$); $q_{ch,cyl}$, chain packing ratio: $q_{ch,cyl} = S_{ch,cyl}/\sigma_{ch}$, σ_{ch} being the cross-sectional area of a molten chain.

View Article Online
DOI: 10.1039/C7TC05315K

inside and between columns, as similarly occurring for rod-like mesogens in the Col$_{hex}$ phases of polycatenar compounds (Figure 3).[45-46]

The values of h$_{mol}$ (columnar slice thickness obtained from the ratio between the molecular volume, V$_{mol}$, and the lattice area, *S*, Table 2) shows a substantial shift from h_π, which indicates a tilted stacking of the flat cores along the columnar axis (by ca. 28-36°, deduced from ratio of h_π and molecular slice thickness h$_{mol}$, Table 2). A further condition for the emergence of columnar mesophases is that the overall cross-sectional area of the peripheral chains is compatible with the interface area offered by stacked mesogens, i.e. that the ratio $q_{ch,cyl}$ of both areas does not deviate too much from unity.[47-48] This ratio is indeed lying between 1.02 and 1.08, meaning that the chains are compactly packed and quasi-stretched, close to well-defined interfaces. Such nearly ideal packing is however the result of the self-optimization of the molecular organization, the interface expansion just required by chains being reached through the tilting of the mesogens out of the columnar plane ($\psi \approx$ 28-36°). This strongly cohesive, rotated and tilted packing (Figure 3) combines with the periodicities of several mesogens along and between neighboring columns, and explains the appearance of additional broad signals D$_1$, D$_2$ from a local-range three-dimensional superstructure. It must be stressed that this model is just a schematic view of how molecules may stack by compromising the average tilt and the hexagonal symmetry. The bulkiness of the sulphur atoms prevents configurations with exact superposition of stacked mesogens, which could be at the origin of the shifts and the rotations along the columns, and ultimately of their average cylindrical shape and of their arrangement into the hexagonal lattice.

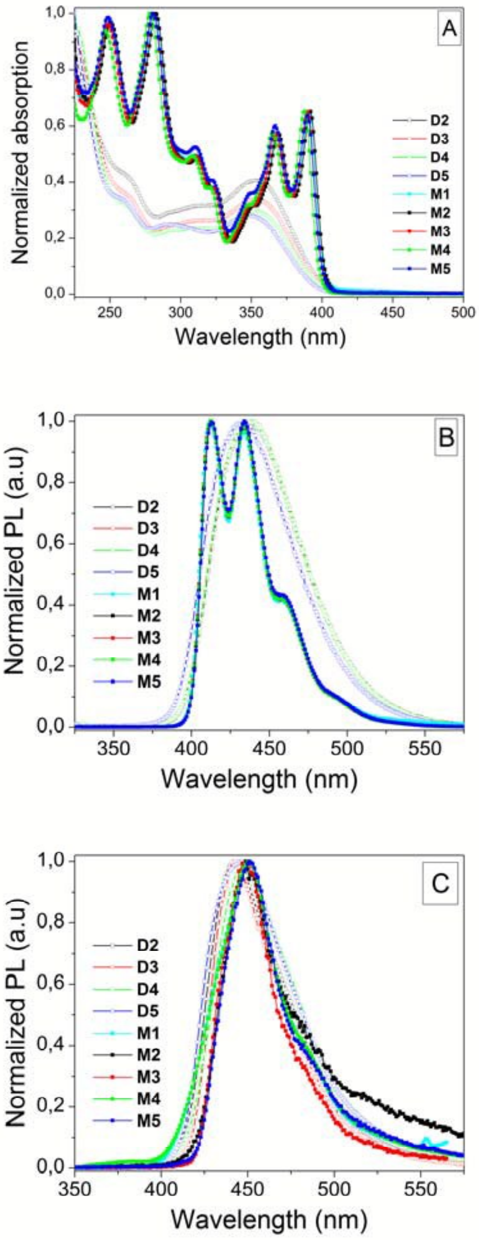

Figure 4. UV/Vis absorption spectra (A), photoluminescence in diluted solution (B) and in solid thin-films (C), respectively, of compounds **D** (open symbols) and **M** (filled symbols).

UV-Vis absorption and photoluminescent properties

The synthesized H-shaped sanidic compounds are large π-conjugated polycyclic aromatic hydrocarbon (PAHs) and as expected show strong light absorption and photo-induced light emission, as measured by UV/vis absorption and photoluminescence (Figure 4 and Table 3).

The main, broad absorption of compounds **D2**-**5** in solution is located below 400 nm. In contrast, the fused compounds **M1**-**5** display two fine, well-resolved absorption bands with four peaks, all located below 400 nm. The absorption spectra of all fused compounds are red-shifted and increased in intensity (molar coefficient), due to the π-conjugated system extension. The thin-film photoluminescence of all compounds is constituted of only one broad and intense peak, located between 430~444 nm for **D2**-**5**, and at 450 nm with a shoulder and long tail for **M1**-**5**. However, the solution photoluminescence of **M1**-**5** is better resolved and exhibit three separated peaks, blue-shifted compared to their film emissions. They emit blue light in THF solution. The light-emitting efficiency (quantum yield, QY) was measured for both series: the tetraaryl-substituted compounds **D** display lower quantum yields, around 10%, than the fused aromatics **M**, which show higher photoluminescence, with efficiency of about 23%. The alkyl chain length do not seem to impact on the photoluminescence of the fused mesogens.

It is conventional that the solid-state emission is red-shifted compared to the emission of the samples in diluted solution, due to the molecular aggregation in the former, resulting in orbital overlap and therefore narrowed HOMO-LUMO energy gap. The fused aromatics **M** compounds display emission QY values higher than that of the **D**-compounds, which can be explained by the difference of the aromatic cores and the decrease of the conjugation. Another factor contributing to the lowering of the QY of compounds **D** might be due to the tetraaryl groups surrounding the thienothiophene core that rotate around the Ar-Ar' sigma bonds in solution, such rotating motions forcing the molecules to relax from excited to ground states, and causing partially fluorescence quenching.

View Article Online
DOI: 10.1039/C7TC05315K

Table 3. Photo-physical properties of the BTBT-containing compounds. Quantum yields were measured with solution concentration of 1×10^{-5} mol L^{-1} in THF excited at 300 nm.

	λ_{abs} (nm)	ε (L mol^{-1} cm^{-1})	λ_{em} solution	λ_{em} film	Solution QY (%)
D2	355	4.05 x 10^4	437	444	9.90
D3	354	3.38 x 10^4	437	443	9.28
D4	353	2.91 x 10^4	437	445	8.90
D5	353	2.94 x10^4	437	438	12.44
M1	248	9.79 x 10^4	412	450	21.30
	280	9.93 x 10^4	434		
	365	5.86 x 10^4	460		
	391	6.54 x10^4			
M2	249	9.73 x 10^4	412	450	22.78
	280	9.96 x 10^4	434		
	367	5.83 x 10^4	460		
	390	6.40 x 10^4			
M3	249	9.73 x 10^4	412	450	22.23
	280	9.96 x 10^4	434		
	367	5.83 x 10^4	460		
	390	6.40 x 10^4			
M4	249	9.73 x 10^4	412	450	22.50
	280	9.96 x 10^4	434		
	367	5.83 x 10^4	460		
	390	6.40 x 10^4			
M5	249	9.73 x 10^4	412	450	21.91
	280	9.96 x 10^4	434		
	367	5.83 x 10^4	460		
	390	6.40 x 10^4			

Charge carrier mobility

As seen above, all thieno[3,2-b]thiophene-fused molecules **M1**-**5** display a hexagonal columnar mesophase with a high clearing temperatures, and a strong tendency for alignment (Figure S10 in SI). They are therefore expected to possess good electronic transport properties. The transient photocurrent time-of-flight (TOF) technique was used here as a direct, simple, and reliable method to obtain both electron and hole mobilities of the liquid crystalline materials and to measure the charge transport mobility rates.

For the measurement of the charge carrier mobility, **M4** was chosen as a representative example. The liquid crystal cell for the TOF study (cell thickness is 16.4 μm) was filled by capillary attraction from the isotropic liquid phase (ca 260°C). The cell, consisting of two ITO glasses sandwiching **M4** sample, was then slowly cooled from the isotropic liquid to guaranty a good homeotropic alignment of the sample into mono-domain. An electric field strength of 20000~50000 V cm^{-1} was applied. The results are shown in Figure 5: i) the transient photocurrent decay curves of holes and electrons with an N_2 laser (337 nm) irradiation are shown in Figure 5A-B; ii) the double-logarithm plots Figure 5C-D were used to directly read out the transit time of charge carriers for mobility calculation (the non-dispersed photocurrent decay curves for both holes and electrons imply the high purity of the liquid crystal sample and the good eletrochemical stability); and iii) Figure 5E-F demonstrate that between 230~100^{o}C, both electron and hole mobility were higher than 10^{-3} cm V^{-1} s^{-1}. Below 100^{o}C, the sample starts to crystallize in the cell (Figure S10) and, poly-crystalline grain boundaries start to form, which act as deep traps for charge carriers, and a dispersed transient photocurrent curve is observed. The TOF charge mobility of **M4** is located in the range of 10^{-4} ~ 0.1 cm^2 V^{-1} s^{-1}, similar to the charge transport rate for reported other one-dimensional columnar mesophases. The columnar phase of this thiophene-fused mesogen therefore acts as an ambipolar semiconductor as both electron and hole mobilities have been realized.

One-dimensional semiconductor made from discotic columnar mesogenic materials normally show TOF mobility in the range of 10^{-4} to 10^{-1} cm^2 V^{-1} s^{-1}. According to the Marcus's theory,[37] the kinetics of electronic charge carrier hopping between two identical molecules, in small molecular semiconductors, is determined by two parameters: i) the reorganization energy and ii) the charge transfer integral, which are both related to the molecular structure and crystalline or supramolecular morphology. As predicted in the Marcus theory, larger π-conjugated aromatics possess lower reorganization energies and higher electronic transfer integrals, therefore higher rates of charge hopping must be displayed.

The SAXS results of the pseudo-discotic mesogens **M1**-**5** show aromatic core-core separations in the 3.7-3.8 Å range in the columns (h_π, Table 2), much larger than the 3.5 Å found for the stacking of conventional discotic systems (e.g. triphenylenes).[51] Such a large spacing implies obviously lesser degree of orbital overlap, and consequently lower carrier mobility. As shown above, this large

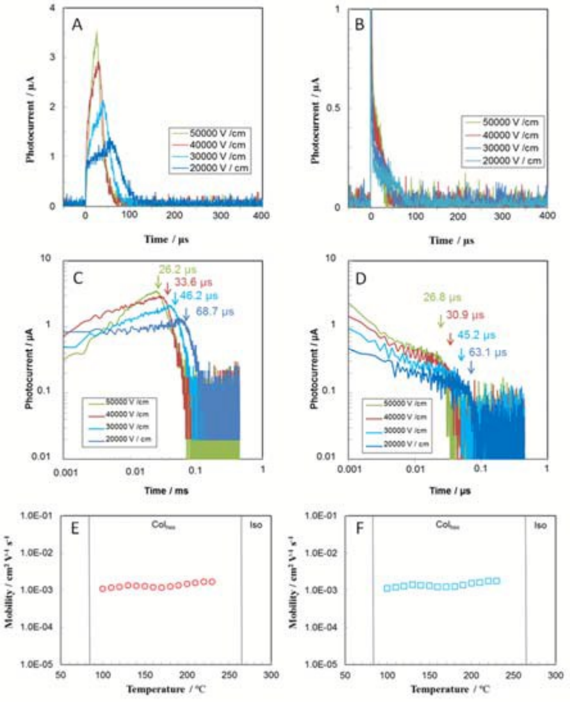

Figure 5. Charge carrier mobility of **M4** measured by TOF technique (at 120°C): A, Transient photo-current (hole) decay cures; B, Transient photo-current (electron) decay curve; C, Double-logarithm plot of hole transport decay curves; D, Double-logarithm plot of electron transport decay curves; E,F, Temperature-dependence of hole mobility and electron mobility.

View Article Online
DOI: 10.1039/C7TC05315K

separation is due to unfavorable factors such as the molecular shape, which possesses two void areas in the centre, and the molecular rotation in the column, which overall result in the decrease of charge transport magnitude.

Despite the modest values of the charge mobility presented by this family of compound, this new molecular system presents however some favorable features that can be further optimized by molecular design, such as an enlarged π-conjugated system and the [1]benzothieno[3,2-b][1]benzothiophene substructure (BTBT),[6,29-32] which otherwise possesses the highest carrier mobility recorded in crystalline and liquid crystalline phases. The synthesized mesogen **M4** compared with conventional BTBT has larger π-conjugated system, smaller reorganization energy and higher charge carrier mobility, according to the Marcus theory predictions.[37,38] The other beneficial factor for charge transport property is the strong tendency for homeotropic alignment of this material in the liquid crystal cell with thickness of 16.4 μm (Figure S10 SI), which provides the long range charge carrier hopping along the discotic molecular column. In summary, the molecular design of these new BTBT-substructure-containing columnar mesogen has been successful as **M4** displays unambiguous hole and electron transport ability in the mesomorphosu temperature range.

Conclusions

Five BTBT-unit containing H - shaped sanidic mesogen have been successfully synthesized by Suzuki cross-coupling reaction and $FeCl_3$ oxidative intermolecular and/or intramolecular Scholl cyclodehydrogenation recation. These π-extended liquid crystals were isolated by simple filtration and purified by crystallization from organic solvent. These mesogens self-organize into hexagonal columnar mesophases with high clearing temperatures and broad mesophase temperature ranges. They emit blue light in THF solution with quantum yield of about 20%. The charge carrier mobility of **M4**, chosen as a representative example, measured by the photocurrent transient TOF technique reveals ambipolar transport properties with equal rate, and values in the range of 10^{-3} cm^2 V^{-1} s^{-1}. Such extended thieno[3,2-b]thiophene-fused columnar mesogens may play an important role in potential applications as organic optoelectronic devices and ambipolar semiconductors.

Acknowledgements

This work was financially supported by the National Nature Science Foundation of China (grant No. 51773140) and a NSFC-JSPS joint project (grant no. 50811140156). BD and BH thank CNRS and Université de Strasbourg for support.

References

1. H. E. Katz, Z. Bao and S. L. Gilat, *Acc. Chem. Res.*, 2001, **34**, 359-369.
2. A. R. Murphy and J. M. J. Frechet, *Chem. Rev.*, 2007, **107**, 1066-1096.
3. C. Wang, H. Dong, W. Hu, Y. Liu and D. Zhu, *Chem. Rev.*, 2012, **112**, 2208-2267.
4. M. E. Cinar and T. Ozturk, *Chem. Rev.*, 2015, **115**, 3036-3140.
5. A. Mishra, C.-Q. Ma and P. Bauerle, *Chem. Rev.*, 2009, **109**, 1141-1276.
6. K. Takimiya, I. Osaka, T. Mori and M. Nakano. *Acc. Chem. Res.*, 2014, **47**, 1493-1502.
7. (a) Y. Geng, A. Fechtenkotter and K.Mullen, *J. Mater. Chem.*, 2001, **11**, 1634-1641; (b) T. Yasuda, H. Ooi, J. Morita, Y. Akama, K. Minoura, M. Funahashi, T. Shimomura and T. Kato, *Adv. Funct. Mater.*, 2009, **19**, 411-419; (c) M. Prehm, G. Gotz, P. Bauerle, F. Liu, X. Zeng, G. Ungar and C. Tschierske, *Angew Chem Int. Ed.*, 2007, **46**, 7856-7859. (e) N. Hu, R. Shao, Y. Shen, D. Chen, N. A. Clark and D. M. Walba, *Adv. Mater.*, 2014, **26**, 2066-2071.
8. (a) C. Xia, X. Fan, J. Locklin and R. Advincula, *Org. Lett.,* 2002, **12**, 2067-2070; (b) W. J. Mitchell, N. Kopidakis, G. Rumbles, D. S. Ginley and S. E. Shaheen, *J. Mater. Chem.*, 2005, **15**, 4518-4528; (c) F. Lincker, B. Heinrich, R. De Bettignies, P. Rannou, J. Pécaut, B. Grévin, A. Pron, B. Donnio and R. Demadrille, *J. Mater. Chem.*, 2011, **21**, 5238-5247; (d) W. W. H. Wong, C.-Q. Ma, W. Pisula, A. Mavrinskiy, X. Feng, H. Seyler, D. J. Jones, K. Mullen, P. Bauerle and A. B. Holmes. *Chem. Eur. J.*, **2011**, 17, 5549-5560.
9. (a) I. Mcculloch, M. Heeney, C. Bailey, K. Genevicius, I. Macdonald, M. Shkunov, D. Sparrowe, S. Tierney, R. Wagner, W. Zhang, M. L. Chabinyc, R. J. Kline, M. D. Mcgehee and M. F. Toney, *Nature Mater.*, 2006, **5**, 328-333; (b) D. Zeng, I. Tahar-Djebbar, Y. Xiao, F. Kameche, N. Kayunkid, M. Brinkmann, D. Guillon, B. Heinrich, B. Donnio, D. A. Ivanov, E. Lacaze, D. Kreher, F. Mathevet, A.-J. Attias, *Macromolecules*, 2014, **47**, 1715-1731
10. L. Chen, S. R. Puniredd, Y.-Z. Tan, M. Baumgarten, U. Zschieschang, V. Enkelmann, W. Pisula, X. Feng, H. Klauk and K. Mullen, *J. Am. Chem. Soc.*, 2012, **134**, 17869-17872.
11. Q. Xiao, T. Sakurai, T. Fukino, K. Akaike, Y. Honsho, A. Saeki, S. Seki, K. Kato, M. Takata and T. Aida, *J. Am. Chem. Soc.*, 2013, **135**, 18268-18271.
12. A. C. Grimsdale, K. L. Chan, R. E. Martin, P. G. Jokisz and A. B. Holmes, *Chem. Rev.*, 2009, **109**, 897-1091.
13. R. K. Gupta, B. Pradhan, S. K. Pathak, M. Gupta, S. K. Pal and A. A. Sudhakar, *Langmuir*, 2015, **31**, 8092-8100.
14. A. Demenev, S. H. Eichhorn, T. Taerum, D. F. Perepichka, S. Patwardhan, F. C. Grozema, L. D. A. Siebbeles and R. Klenkler, *Chem. Mater.*, 2010, **22**, 1420-1428.
15. D. M. Knawby and T. M. Swager, *Chem. Mater.*, 1997, **9**, 535-538.
16. M. J. Cook and A. Jafari-Fini, *J. Mater. Chem.*, 1997, **7**, 5-7.
17. M. J. Cook and A. Jafari-Fini, *Tetrahedron*, 2000, **56**, 4085-4094.
18. A. D. Bromby, W. H. Kan and T. C. Sutherland, *J. Mater. Chem.*, 2012, **22**, 20611-20617.
19. H. Suzuki, K. Kawano, K. Ohta, Y. Shimizu, N. Kobayashi and M. Kimura, *Chem. Open*, 2016, **5**, 150-156.
20. J. Luo, B. Zhao, H. S. O. Chan and C. Chi, *J. Mater. Chem.*, 2010, **20**, 1932-1941.
21. J. Luo, B. Zhao, J. Shao, K. A. Lim, H. S. O. Chan and C. Chi, *J. Mater. Chem.*, 2009, **19**, 8327-8334.
22. Q. Ye, J. Chang, K.-W. Huang and C. Chi, *Org. Lett.*, 2011, **13**, 5960-5963.
23. T. Kato, M. Yoshio, T. Ichikawa, B. Soberats, H. Ohno and M. Funahashi, *Nat. Rev. Mater.*, 2017, **2**, 17001.
24. T. Wöhrle, I Wurzbach, J. Kirres, A. Kostidou, N. Kapernaum, J. Litterscheidt, J. C. Haenle, P. Staffeld, A. Baro, F. Giesselmann and S. Laschat, *Chem. Rev.*, 2016, **116**, 1139-1241.
25. B. R. Kaafarani, *Chem. Mater.*, 2011, **23**, 378-396.
26. S. Sergeyev, W. Pisula and Y. H. Geerts, *Chem. Soc. Rev.*, 2007, **36**, 1902-1929.

View Article Online
DOI: 10.1039/C7TC05315K

27. Y. Shimizu, K. Oikawa, K. Nakayama and D. Guillon, *J. Mater. Chem*., 2007, **17**, 4223-4229.
28. M. Funahashi and T. Kato, *Liq. Cryst*., 2015, **42**, 909-917.
29. S. Mery, D. Haristoy, J. Nicoud, D. Guillon, S. Diele, H. Monobe and Y. Shimizu, *J. Mater. Chem*., 2002, **12**, 37-41.
30. H. Monobe, L. L. An, P. Hu, B. Q. Wang, K. Q. Zhao and Y. Shimizu, *Mol. Cryst. Liq. Cryst*., 2017, **647**, 119-126.
31. H. Iino, T. Usui and J. Hanna, *Nat. Comm*., 2015, **6**, 6828.
32. L. Mazur, A. Castiglione, K. Ocytko, F. Kameche, R. Macabies, A. Ainsebaa, D. Kreher, B. Heinrich, B. Donnio, S. Sanaur, E. Lacaze, J.-L. Fave, K. Matczyszyn, M. Samoc, J. Weon Wu, A.-J. Attias, J.-C. Ribierre and F. Mathevet, *Org. Electr.*, 2014, **15**, 943-953.
33. K. Q. Zhao, M. Jing, L. L. An, J. Q. Du, Y. H. Wang, P. Hu, B. Q. Wang, H. Monobe, B. Heinrich and B. Donnio, *J. Mater. Chem. C*, 2017, **5**, 669-682.
34. K. Q. Zhao, L. L. An, X. B. Zhang, W. H. Yu, P. Hu, B. Q. Wang, J. Xu, Q. D. Zeng, H. Monobe, Y. Shimizu, B. Heinrich and B. Donnio, *Chem. Eur. J*., 2015, **21**, 10379-10390.
35. K. Q. Zhao, J. Q. Du, X. H. Long, M. Jing, B. Q. Wang, P. Hu, H. Monobe, B. Henrich and B. Donnio, *Dyes Pigm*., 2017, **143**, 252-260.
36. K. Q. Zhao, C. Chen, H. Monobe, P. Hu, B. Q. Wang and Y. Shimizu, *Chem. Commun*., 2011, **47**, 6290-6292.
37. R. A. Marcus, *Rev. Mod. Phys*., 1993, **65**, 599-610.
38. V. Lemaur, D. A. da Silva Filho, V. Coropceanu, M. Lehmann, Y. Geerts, J. Piris, M. G. Debije, A. M. van de Craats, K. Senthilkumar, L. D. A. Siebbeles, J. M. Warman, J. L. Bredas and J. Cornil, *J. Am. Chem. Soc*., 2004, **126**, 3271-3279.
39. C. Feng, X. Wang, B. Q. Wang, K. Q. Zhao, P. Hu and Z. J. Shi, *Chem. Commun*., 2012, **48**, 356-358.
40. C. Feng, X. L. Tian, J. Zhou, S. K. Xiang, W. H. Yu, B. Q. Wang, P. Hu, C. Redshaw and K. Q. Zhao, *Org. Biomol. Chem*., 2014, **12**, 6977-6981.
41. C. Feng, Y. H. Ding, X. D. Han, W. H. Yu, S. K. Xiang, B. Q. Wang, P. Hu, L. C. Li, X. Z. Chen and K. Q. Zhao, *Dyes Pigm*., 2017, **139**, 87-96.
42. X. D. Han, X. L. Tian, W. H. Yu, S. K. Xiang, P. Hu, B. Q. Wang, K. Q. Zhao, X. Z. Chen and C. Feng, *Liq. Cryst*., 2017, **44**, 1727-1738.
43. K. Q. Zhao, X. Y. Bai, B. Xiao, Y. Gao, P. Hu, B. Q. Wang, Q. D. Zeng , C. Wang, B. Heinrich and B. Donnio, *J. Mater. Chem. C*, 2015, **3**, 11735-11746.
44. K. Q. Zhao, Y. Gao, W. H. Yu, P. Hu, B. Q. Wang, B. Heinrich and B. Donnio. *Eur. J. Org. Chem*., 2016, 2802-2814.
45. A. C. Ribeiro, B. Heinrich, C. Cruz, H. T. Nguyen, S. Diele, M. W. Schröder and D. Guillon, *Eur. Phys. J. E*, 2003, **10**, 143-151.
46. B. Donnio, B. Heinrich, H. Allouchi, J. Kain, S. Diele, D. Guillon and D. W. Bruce, *J. Am. Chem. Soc.*, 2004, **126**, 15258-15268.
47. D. Mysliwiec, B. Donnio, P. J. Chmielewski, B. Heinrich and M. Stepien, *J. Am. Chem. Soc*., 2012, **134**, 4822-4833.
48. B. Alameddine, O. F. Aebischer, B. Heinrich, D. Guillon, B. Donnio and T. A. Jenny, *Supramol. Chem*., 2014, **26**, 125-137.
49. The Cambridge Structural Database. T. L. Andresen, F. C. Krebs, N. Thorup and K. Bechgaard, *Chem. Mater.*, 2000, **12**, 2428-2433.
50. The Cambridge Structural Database. E. G. Cox, R. J. J. H. Gillot and G. A. Jeffrey, *Acta Crystallogr.*, 1949, **2**, 356-363.
51. S. Kumar, *Chem. Soc. Rev*., 2006, **35**, 83-109.

Facile Synthesis of Benzothienobenzothiophene-Cored Columnar Semiconductor Mesogens